

# ORIGIN OF DOLOMITE IN THE MIDDLE TRIASSIC ZHOUCHEGONGCUN FORMATION, CENTRAL LOWER YANGTZE REGION, SOUTHEAST CHINA

**Qing LI<sup>1,2</sup>, Zaixing JIANG<sup>1</sup>, Wenxuan HU<sup>3</sup> & Xuelian YOU<sup>4</sup>**

<sup>1</sup>*School of Energy Resources, China University of Geosciences, Beijing 100083, PR China, e-mail: tsinglee2659@gmail.com*

<sup>2</sup>*Department of Geosciences, The Pennsylvania State University, University Park, PA 16802, USA, e-mail: qul15@psu.edu*

<sup>3</sup>*State Key Laboratory for Mineral Deposits Research, School of Earth Sciences and Engineering, Nanjing University, Nanjing 210093, PR China, e-mail: huwx@nju.edu.cn*

<sup>4</sup>*School of Ocean Sciences, China University of Geosciences, Beijing 100083, PR China, e-mail: youxuelian007@gmail.com*

**Abstract:** The Middle Triassic Zhouchongcun Formation (correlated to the Anisian stage by global standards) in the Lower Yangtze region is mainly composed of limestones that have been partially to completely dolomitized. However, the origin of these dolomites and the nature of dolomitization fluid have not been well documented. The Geshan section, a typical section dealing with the Middle Triassic dolomite of the Lower Yangtze region, was chosen as the research object in this study. The dolomite in the Zhouchongcun Formation from Geshan section commonly displays planar-e texture and locally planar-s texture with crystal sizes up to 80 $\mu$ m. These dolomites commonly contain residual calcites inclusions in their crystals and the development of dolomite is associated with stylolites, indicating that this dolomite formed by replacement and the dolomitization occurred at burial depth of more than 500m. The dolomites have a narrow range of  $\delta^{13}\text{C}$  values (from 5.4‰ to 7.2‰, V-PDB), which are partly overlapped with the theoretical  $\delta^{13}\text{C}$  value of seawater dolomite and show slightly enrichment. The narrow range and positive  $\delta^{13}\text{C}$  values suggest that the influence of fluid with isotopically light  $\delta^{13}\text{C}$  was negligible in the dolomitization. The large overlap of  $^{87}\text{Sr}/^{86}\text{Sr}$  ratios of the dolomites with the coeval Triassic seawater suggests that the dolomitizing fluids may have derived from modified Triassic seawater preserved in formations. In comparison with Triassic seawater dolomite, the Geshan dolomite has depleted of  $\delta^{18}\text{O}$  values (-8.4‰ to -6.5‰, V-PDB) and low Sr but high Fe, Mn concentration and Ce/Ce\* ratios, suggesting that dolomitization occurred in an anoxic subsurface environment with increasing temperature during compaction at shallow to intermediated burial. The Ce/Ce\* ratio and  $\Sigma\text{REE}+\text{Y}$  contents of Zhouchongcun carbonate increase with depth, reflecting that the environment becoming more anoxic and having higher temperature with the deeper burial depth. Based on the burial history of the Lower Yangtze region, the dolomitization most likely occurred during the Late Triassic period.

**Keywords:** Dolomite, isotope, trace elements, REE, seawater

## 1. INTRODUCTION

Dolomites account for approximately half of all carbonate rocks and dolomite reservoirs comprise one of the most important reservoirs in marine petroliferous basins (Sun, 1995). The formation of dolomite has been extensively studied in carbonate sedimentology (e.g. Qing & Mountjoy, 1989, Warren, 2000; Azmy et al., 2001). Numerous models of dolomitization have been proposed to explain the

widespread dolomites, including sabkha-style dolomitization (Mackenzie, 1981), bacterial mediation dolomitization (You et al., 2013); dolomitization by sea water (Land, 1985; ); brine reflux dolomitization (Jones & Xiao, 2005); dolomitization in a seawater/meteoric water mixing zone (Fookes, 1995); burial dolomitization (Wierzbicki et al., 2006); hydrothermal dolomitization (Davies & Smith, 2006). However, the origin of ancient massive dolomites and the nature of

dolomitization fluid have still been some of the most intensively debated (Kirmaci & Akdag, 2005).

Carbonate occurs pervasively in the Yangtze region during Lower and Middle Triassic period and is considered as a potential regional hydrocarbon exploration target (Wang et al., 2014b). Extensive studies have been performed on dolomitization in the Upper Yangtze region (e.g. Ma et al., 2008). However, the origin of dolomite developed in the Lower Yangtze region during Triassic has not been well documented (Wang et al., 2014a). As some evaporite beddings were found in the upper part of the Zhongchongcun Formation (Hu et al., 2008), the dolomites were simply thought to be formed penecontemporaneously under Sabkha conditions or by seepage refluxed brine (Wang et al., 2014a; 2014b). However, we found that dolomite developed at Geshan section was related to stylolites, which were commonly considered to form at late diagenesis stage (Kirmaci & Akdag, 2005; Wierzbicki et al., 2006). Obviously, the origin of the Middle Triassic dolomite in the Lower Yangtze region and the condition under which dolomitization took place are not fully understood. The nature of the dolomitization fluids is still blur and needs to be clarified.

On the basis of petrographic and geochemical data, the major objectives of this study are to: 1) define the petrography and geochemistry signatures of dolomite in the Geshan section Zhouchongcun Formation; 2) constrain the origin and nature of dolomitizing fluids and dolomitizing environment;

3) determine the burial history and the timing of dolomitization.

## 2. GEOLOGICAL SETTING

The Lower Yangtze region, located in the east of the Yangtze plate, southeastern China (Fig. 1A), is one of the important marine sedimentation areas of petroleum distribution in southern China (Huang et al., 2012).

Extensive carbonate deposits were developed during the Early and Middle Triassic periods in the Lower Yangtze Region. The Lower Triassic strata are mainly composed of carbonate deposit (Fig. 1B), with the thickness up to 1200m (Wang & Duan, 2009). During the Middle Triassic, the sedimentary facies were mainly lagoon (Liu & Tong, 2001). The Middle Triassic strata comprises a variety of lithologies, including limestone, dolomitic limestone, dolomite, and anhydrite (Fig. 1B), indicating a salty environment (Wang et al., 2014a).

The Middle Triassic is a special period during the evolutionary history of sedimentary basins in southern China. The depositional environments of the Lower Yangtze region transformed from marine environment to paralic environment, and eventually becoming continental deposits during this period (Liu & Tong, 2001). Although the global sea level has been rising during the Middle Triassic, the relative sea level in the Lower Yangtze region was declining due to the tectonic uplift (Hu et al., 2008).

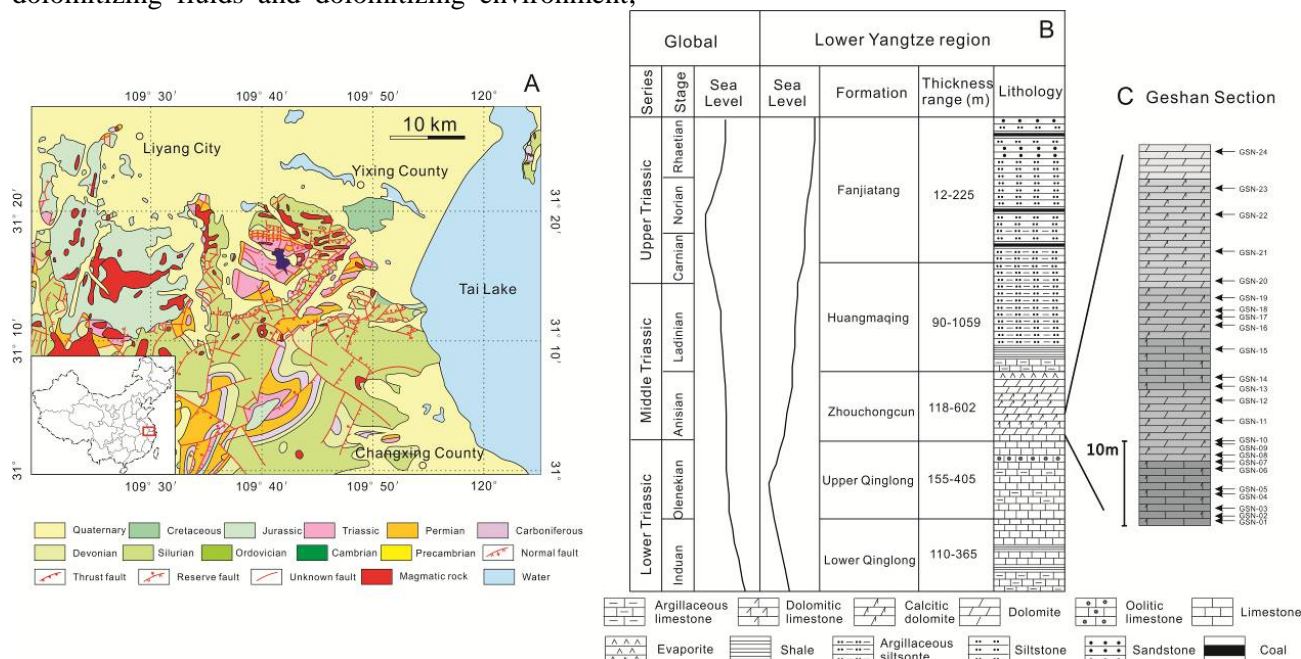


Figure 1. (A) Tectonic setting and geological units of the Yixing area in Lower Yangtze region, south-east China and the location of Geshan section (blue pin) (modified after Wang et al., 2014b). (B) Correlation between the Yixing area and global standards (modified after Hu et al., 2008). And stratigraphic and lithologic succession of the Triassic strata in the study area. (C) General lithology column of the Geshan section and the locations of collected samples.

The climate in the Lower Yangtze region changed from tropical climate during the Early Triassic to subtropical arid climate during the Middle Triassic, and then transformed into a warm and humid climate during the Late Triassic (Wang et al., 2014a).

The Geshan section, a well-exposed section, was selected as the research object in this study. It is located in southwest of Yixing City, Jiangsu Province, China (Fig. 1A) and is a typical section for study of the Middle Triassic dolomite in the Lower Yangtze region (Wang et al., 2014a, 2014b). The outcropping rocks of this section are predominantly carbonates of lower part of the Zhouchongcun Formation, Middle Triassic (Fig. 1C). The lithologies are mainly composed of dolomite and partly dolomitized limestones (Fig. 1C). Biostratigraphic data shows that the Zhouchongcun Formation in the Lower Yangtze region was correlated to the Anisian stage of Middle Triassic by global standards (Fig. 1B) (Hu et al., 2008).

### 3. METHODS

A total of 24 samples were collected from the Geshan section for petrographic analyses (Fig. 1C). Dolomites from 12 specimens were selected and sampled using a dental drill for carbon, oxygen, strontium isotope, trace elements, and rare earth elements (REE) analysis. The analyses were performed at the State Key Laboratory for Mineral Deposits Research, Nanjing University. Thin sections were partly stained with Alizarin Red S and K-ferricyanide for carbonate mineral determination.

Electron probe microanalyses (EPMA) were carried out on polished, carbon-coated thin section using a JEOL JXA-8100 electron microprobe with a wavelength-dispersive system. It was operated with three crystal spectrometers, and with accelerating voltage of 15 kV and specimen current of 20nA. The detection limits of the microprobe were estimated at approximately 0.002 element %.

For stable carbon and oxygen isotope analyses, the powdered micro-samples (50 mg) were reacted with 100% orthophosphoric acid at 50°C for 3 h under vacuum to produce CO<sub>2</sub> gas. The carbon and oxygen ratios of the equilibrated CO<sub>2</sub> gas were determined on a Finnigan MAT-252 mass spectrometer. The analytical precision is better than 0.1%. The isotope data are reported in the standard notation relative to standard V-PDB.

For trace elements and REE content analyses, 50 mg ( $\pm 0.2$ mg) of dolomite micro-samples were

precisely weighed and were reacted with 5 ml acetic acid with 1 mol/L concentration for 12 h under ultrasound condition in a teflon beaker. After 15 minutes' centrifugation, transfer the upper liquid to another Teflon beaker. The residue was dried and weighed. The weight of the residue was deducted when final calculation the weight of reacted dolomite. The upper liquid was evaporated to dryness and dissolved in 1 ml concentrated nitric acid, and then evaporated to dryness again in order to remove residual acetic acid. Finally, 5 ml nitric acid with the concentration of 1 mol/L and 1 ml standard solution with Rh of  $100 \times 10^{-9}$  (weight percent) was added, and the fluid volume was fixed to 10 ml. The trace elements and REE were determined on a Finnigan MAT-252 ICP-MS. The analytical precision is better than 0.1%. The REE+Y concentrations were normalized against Post Archaean Average Shale (PAAS; Taylor & McLennan, 1985).

A total of 11 samples were analyzed for <sup>87</sup>Sr/<sup>86</sup>Sr ratios. About 150 mg of dolomite rock was finely ground in an agate mortar and pestle prior to chemical dissolution. The dolomite samples were leached by 1 N HCl to remove exchangeable Sr from clays and inter-crystalline calcite. Sr was separated from other cations using 50 AL columns filled with Eichrome Sr-Spec resin. Sr was loaded on Re filaments in a solution of TaCl<sub>5</sub> and H<sub>3</sub>PO<sub>4</sub>, and was analyzed on a MAT 262 multicollector mass spectrometer with a correction ratio of <sup>88</sup>Sr/<sup>86</sup>Sr=8.37521. The Standard NBS 987 was routinely analyzed and yielded a mean value of 0.710254 $\pm$ 12 (2 $\sigma$ ).

## 4. RESULTS

### 4.1 Petrography

The Zhouchongcun Formation in the study area is formed of limestones that have been dolomitized to varying degrees (Fig. 2). Dolomite is commonly reddish gray or pink in color. Dolostones in the Geshan section range from scattered dolomite rhombs to nearly complete dolomite (Fig. 2B and C). The dolomites exhibit planar-e texture and locally planar-s texture with crystal sizes commonly up to 80 $\mu$ m (Fig. 2). Many dolomite crystals contain calcite inclusions in their crystals (Fig. 2D). The dolomites nearest to the pores are more developed than those located far away from the pores (Fig. 2E). The development dolomite is associated with stylolites as the most extensive dolomitization is commonly immediately adjacent to stylolites (Fig. 2F).

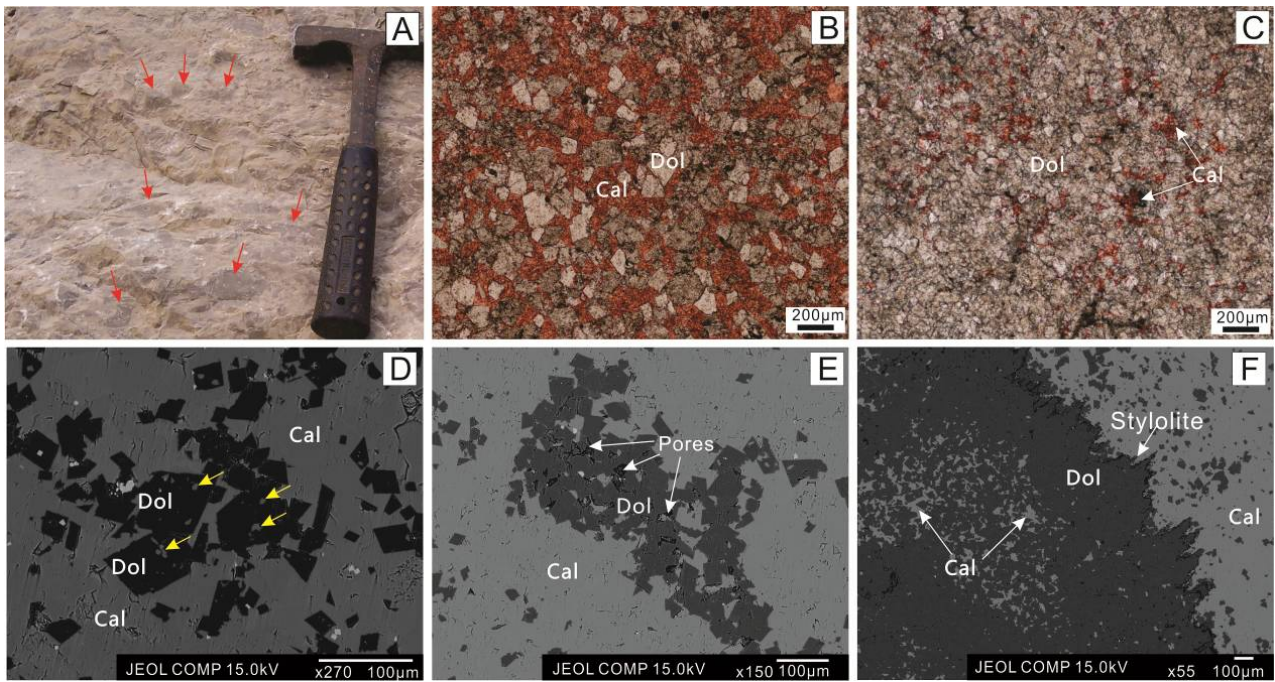


Figure 2. Photomicrographs and back scattered electron images of samples from the Geshan section. (A) Partially dolomitized limestone. The dolomites are reddish gray in color (red arrows); (B) Calcitic dolomite with scattered dolomite rhombs under plane light; (C) Massive dolomite under plane light; (D) Some dolomites contain residual calcites inclusion in their crystals. Back scattered electron image; (E) Dolomite was more developed in porous area. Back scattered electron image; (E) The development dolomite is associated with stylolites. Pervasive dolomite occurred along only one side of stylolites while the other side is less. Back scattered electron image.

#### 4.2 Isotope data

The carbon and oxygen isotopic compositions of the Geshan dolomites are plotted in figure 3 and summarized in table 1. The  $\delta^{13}\text{C}$  and  $\delta^{18}\text{O}$  of the dolostones range from 5.4‰ to 7.2‰ V-PDB (average 6.2‰, n=12) and from -8.4‰ to -6.5‰ V-PDB (average -7.8‰, n=12), respectively. The  $\delta^{13}\text{C}$  composition of the Geshan dolomites is slightly enriched relative to seawater dolomite values (Fig. 3). The  $\delta^{18}\text{O}$  values of these dolomites, however, are distinctly more negative than seawater dolomites (Fig. 3). The strontium isotopic compositions of the Geshan dolomites are presented in Fig 4 and Table 1. These dolostones have  $^{87}\text{Sr}/^{86}\text{Sr}$  ratios from 0.70801 to 0.70819 (n=12) with an average of 0.70810.

#### 4.3 Major and trace elements

The compositions of the Geishan dolomite obtained from EPMA analyses are plotted in figure 5. Sr concentration in dolomite varies from below detection limit (bdl) to 625.7 ppm. The Fe concentration of dolomite ranges from bdl to 4441.1 ppm. The Mn content of dolomite spans from bdl to 317.6 ppm. The Na concentration of dolomite ranges from 22.3 ppm to 712.3 ppm. The Mg/Ca ratio for

dolomite varies between 0.7 and 1.1.

Mn and Sr concentrations obtained from wet chemical analysis are list in table 1. The Sr content of dolomite from the Zhouchongcun Formation ranges from 80.55 ppm to 886.38 ppm (average 240.43 ppm, n=12). The Mn content ranges from 5.20 ppm to 28.02 ppm, with an average of 12.97 (n=12).

#### 4.4 REE

The total REE contents of the Geshan dolomite vary between 0.99 and 7.09 ppm (average=3.35 ppm) and Y between 0.32 and 1.29 ppm (average= 0.71 ppm) (Table. 1). There is no correlation between  $\Sigma\text{REE}+\text{Y}$  and Mn content. The shale -normalized REE +Y distribution patterns derived from the carbonates of Geshan section are characterized by flat REE patterns and low REE contents (Fig. 6A). There are no obvious negative Ce anomalies.  $\text{Ce}/\text{Ce}^*$  values [ $2\text{Ce}_\text{N}/(\text{La}_\text{N}+\text{Pr}_\text{N})$ ] range from 0.82 to 1.08 (average 0.99, n=12). These are not compatible with modern oxygenated seawater (Fig. 6B).  $\text{Pr}/\text{Pr}^*$  [ $2\text{Pr}_\text{N}/(\text{Ce}_\text{N}+\text{Nd}_\text{N})$ ] values range from 0.94 to 1.09 (average 0.98, n=12).  $\text{Eu}/\text{Eu}^*$  [ $2\text{Eu}_\text{N}/(\text{Sm}_\text{N}+\text{Gd}_\text{N})$ ] vary from 0.78 to 1.07 (average=0.91, n=12).  $\text{Nd}_\text{N}/\text{Yb}_\text{N}$  span from 0.70 to 1.09, (average = 0.89, n = 12), indicating a slight LREE depletion.

Table 1 REE + Y concentration ( $\mu\text{g/g}$ ), trace elements concentration (ppm),  $\delta^{13}\text{C}$ ,  $\delta^{18}\text{O}$  value (‰), and  $^{87}\text{Sr}/^{86}\text{Sr}$  ratio of Zhouchongcun dolomites.

Sample	GSN-01	GSN-03	GSN-06	GSN-09	GSN-12	GSN-15	GSN-17	GSN-18	GSN-20	GSN-21	GSN-23	GSN-24
La	0.96	1.37	0.73	0.71	0.67	0.74	0.47	0.72	0.66	0.66	0.43	0.21
Ce	2.05	3.02	1.56	1.46	1.33	1.45	0.93	1.35	1.36	1.11	0.85	0.35
Pr	0.20	0.32	0.15	0.16	0.14	0.15	0.09	0.14	0.15	0.14	0.09	0.05
Nd	0.77	1.25	0.59	0.58	0.48	0.59	0.35	0.55	0.59	0.54	0.39	0.18
Sm	0.15	0.24	0.12	0.12	0.10	0.11	0.07	0.11	0.12	0.12	0.08	0.04
Eu	0.03	0.05	0.03	0.02	0.02	0.02	0.02	0.02	0.02	0.02	0.02	0.01
Gd	0.15	0.24	0.13	0.11	0.11	0.12	0.07	0.10	0.13	0.12	0.09	0.04
Tb	0.02	0.03	0.02	0.02	0.01	0.02	0.01	0.01	0.02	0.01	0.01	0.01
Dy	0.13	0.22	0.11	0.12	0.10	0.11	0.06	0.09	0.10	0.09	0.08	0.05
Y	0.82	1.29	0.74	0.73	0.70	0.79	0.42	0.62	0.75	0.81	0.57	0.32
Ho	0.03	0.04	0.02	0.03	0.02	0.02	0.01	0.02	0.03	0.02	0.02	0.01
Er	0.08	0.14	0.06	0.07	0.06	0.07	0.03	0.05	0.07	0.06	0.04	0.02
Tm	0.01	0.02	0.01	0.01	0.01	0.01	0.01	0.01	0.01	0.01	0.01	0.00
Yb	0.08	0.12	0.06	0.06	0.05	0.06	0.03	0.05	0.04	0.04	0.04	0.02
Lu	0.01	0.02	0.01	0.01	0.01	0.01	0.00	0.01	0.01	0.01	0.01	0.00
$\Sigma\text{REE+Y}$	5.49	8.37	4.34	4.20	3.80	4.26	2.57	3.84	4.07	3.77	2.71	1.31
Ce/Ce*	1.08	1.05	1.07	1.02	1.02	1.01	1.03	0.98	0.99	0.85	0.97	0.82
Pr/Pr*	0.94	0.97	0.95	0.99	1.00	0.95	0.94	0.95	0.99	1.05	0.98	1.09
$\delta^{13}\text{C}$ (‰)	5.8	6.4	6.1	5.7	6.4	7.2	6.9	6.3	5.7	6.1	6.3	6.2
$\delta^{18}\text{O}$ (‰)	-7.0	-7.1	-8.2	-8.4	-7.9	-7.7	-6.5	-8.2	-8.2	-7.9	-7.9	-8.4
Mn (ppm)	15.02	16.68	10.35	10.66	10.95	5.90	5.20	6.83	9.72	28.02	9.85	25.18
Sr (ppm)	140	221	183	173	143	470	886	156	154	113	149	81
$^{87}\text{Sr}/^{86}\text{Sr}$	0.708 168	0.708 191	0.708 092	0.708 095	0.708 118	0.708 041	0.70 8010	0.708 101	0.708 120	0.708 105	-	0.708 117
(2 $\sigma$ )	0.000 010	0.000 010	0.000 012	0.000 013	0.000 011	0.000 011	0.00 0011	0.000 009	0.000 010	0.000 011	-	0.000 013

## 5. DISCUSSION

### 5.1 Interpretation of Petrography

Dolomites contain residual calcites inclusion in their crystals (Fig. 2D), indicating a replacement origin. Extensive dolomite occurred along stylolite indicates that the dolomite clearly postdates the onset of stylolite development. The development of stylolites commonly begins to occur at the depth of about 500-1000m (Lind, 1993; Kirmaci & Akdag, 2005). The geothermal gradient of the study area during the Late Triassic was 3.1°C/100m (Liu, 2004). Assuming that the surface temperature was 30°C (Qing & Mountjoy, 1989), the calculated minimum precipitation temperatures for the replacement dolomite were 45.5°C to 61°C. Some bitumen was filled in intercrystalline pore space (Fig. 2C), indicating that dolomitization occurred before or within the main generation and migrate of petroleum.

### 5.2 Interpretation of isotope data

#### 5.2.1 Carbon isotope

$\delta^{13}\text{C}$  values were usually used to reveal the source of the carbon of carbonate (Veizer et al., 1999). Dolomite was commonly enriched in  $\delta^{13}\text{C}$

with respect to calcite because of the carbon isotope fractionation (Jimenez-Lopez et al., 2006).  $\delta^{13}\text{C}$  value is commonly 2‰ enrich in dolomite than in calcite (Bristow et al., 2012). The  $\delta^{13}\text{C}$  values of low-magnesium shells in Middle Triassic mainly range from 1‰ to 4‰ (V-PDB) (Veizer et al., 1999). Thus, the theoretical  $\delta^{13}\text{C}$  values of seawater dolomite are between 3‰ and 6‰ (V-PDB). The measured  $\delta^{13}\text{C}$  values of Zhouchongcun dolomite, ranging from 5.4‰ to 7.2‰ (V-PDB), are partly overlapped with the theoretical  $\delta^{13}\text{C}$  value of seawater dolomite and show slightly enrichment (Fig. 3).

Carbonate sediments that have undergone mineralogical stabilization in meteoric water associated with subaerial exposure generally have a wide range of  $\delta^{13}\text{C}$  values and are generally depleted in  $\delta^{13}\text{C}$  (Qing & Mountjoy, 1989). In the Geshan section, however, the dolostones have a narrow range of positive  $\delta^{13}\text{C}$  values, suggesting that the influence of fluid with isotopically light  $\delta^{13}\text{C}$  (such as meteoric water and fluid in association with organic matter) was negligible in the dolomitization (Kirmaci & Akdag, 2005). This is also supported by the lack of meteoric cements. Therefore, it is unlikely that these dolomites formed in a mixing-zone environment.

The  $\delta^{13}\text{C}$  values of Geshan dolostones are

partly compatible with values associated with marine dolomites, indicating that the dolomite likely precipitated from seawater or modified seawater stored in pores. The most likely cause of the slightly enriched  $\delta^{13}\text{C}$  value is that this dolomite precipitated at elevated diagenetic temperature, which could influence carbon isotope fractionation between  $\text{HCO}_3^-$  derived from host limestone dissolution and dolomite. Dolomite precipitating from fluids with high temperature would be enriched in  $\delta^{13}\text{C}$  (Barnaby & Read, 1992). On the other hand, positive carbon isotope may also be because these dolomites precipitated in relatively closed diagenesis environment from high salinity brines (Wen et al., 2014).

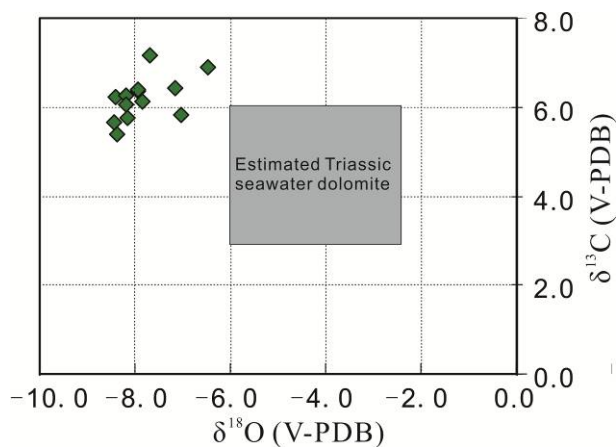


Figure 3. Crossplot of stable carbon and oxygen isotopic value composition for the Geshan dolomites. Estimated stable isotope value of marine dolomite modified after Tritlla et al., 2001.

### 5.2.2 Oxygen isotope

The depletion in  $\delta^{18}\text{O}$  can be caused by the influence of meteoric water (Mresah, 1998) and elevated precipitation temperatures (Barnaby & Read, 1992). The influence of meteoric water is unlikely the reason for the depleted  $\delta^{18}\text{O}$  values of dolomites in the Zhouchongcun Formation, because: 1) meteoric diagenetic fabrics (such as grain dissolution, moldic and vuggy porosities, and meteoric cements) were not observed; 2) The dolomite related to stylolites, indicating a late diagenesis instead of penecontemporaneous or early diagenesis; 3) The positive  $\delta^{13}\text{C}$  value implies that meteoric water was not largely involved in the dolomitization. Thus, the low  $\delta^{18}\text{O}$  values of the Geshan dolomite are mostly because they precipitated at elevated temperature.

### 5.2.3 Strontium isotope data

Strontium isotope data of dolomite are generally used to define dolomitization fluid as

$^{87}\text{Sr}/^{86}\text{Sr}$  signatures yielded by dolomite bodies commonly reflect the dolomitizing fluids rather than the precursor limestone (Zhao & Jones, 2012). The Sr isotopic composition of seawater has evolved over geological time (Fig. 4) (Veizer et al., 1999). The large overlap of  $^{87}\text{Sr}/^{86}\text{Sr}$  ratio of the Geshan dolomites from lower Zhouchongcun Formation with the coeval Triassic seawater suggests that the dolomitizing fluids may have derived from the connate seawater preserved in the formation. The slight increase in  $^{87}\text{Sr}/^{86}\text{Sr}$  ratio was probably induced by enhanced water-rock interaction (Azmy et al., 2001).

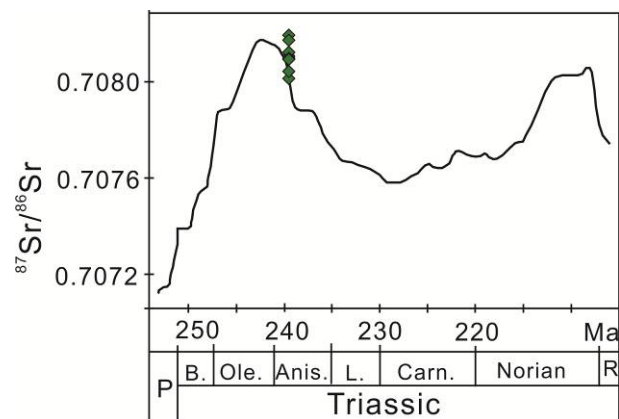


Figure 4.  $^{87}\text{Sr}/^{86}\text{Sr}$  ratio of the Geshan dolomite and their comparison with the Triassic seawater Sr composition/time curve (modified after Korte et al., 2003).

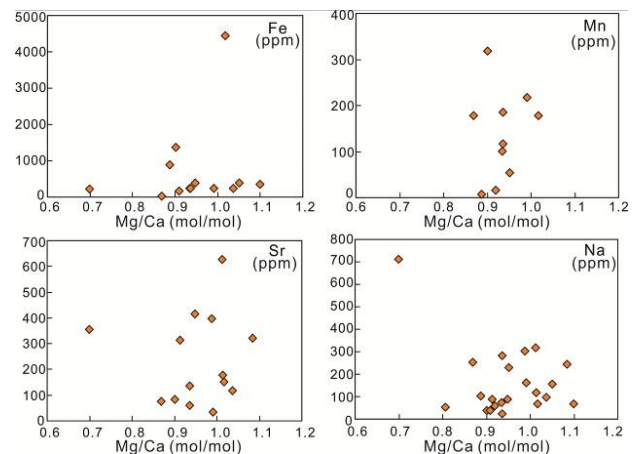


Figure 5. Fe-, Mn-, Sr-, and Na-content vs. Mg/Ca ratio of the Geshan dolomite

### 5.3 Interpretation of trace elements

Dolomites commonly contain lower Sr concentration relative to limestones due to the smaller Sr partitioning coefficient in dolomite (Veizer, 1983; Qing & Mountjoy, 1989). According to the dolomite-water distribution coefficient,

dolomites formed in normal seawater should have a theoretical equilibrium concentration of 470 to 550 ppm Sr (Veizer, 1983). Most fine crystalline “penecontemporaneous” dolomites from evaporitic environments have about 500 to 700 ppm Sr (Land, 1991). The dolomites in the Geshan area have a low range of Sr concentration (Fig. 5).

Assuming bulk solution equilibrium, the low Sr concentration in the Geshan dolomites suggests that these dolomites were not precipitated in an evaporitic or normal marine environment. The low Sr concentration in the dolomites was likely caused by purification of dolomite during recrystallization under burial condition (e.g., Kirmaci & Akdag, 2005).

The equilibrium concentrations of Mn in carbonate precipitated from seawater are approximately 1 ppm on average (Veizer, 1983). When meteoric waters involved in carbonate diagenesis, Mn concentrations could be up to 34000 ppm (Driese & Mora, 1993). The Mn concentration in Geshan dolomites is much lower than that in meteoric water related carbonate, indicating that invasion of meteoric water had negligible influence on dolomitization in the Zhongchongcun Formation. As the Mn element can be more easily incorporated into dolomite lattice under reducing conditions (Smith, 2006), the slightly higher contents of Mn elements in Geshan dolomites than in seawater dolomite suggests that these dolomites were precipitated from fluids enriched in Mn elements under reducing conditions, supporting a subsurface origin as the burial diagenesis of carbonates is a process with Fe and Mn enrichment and strontium depletion (Veizer, 1983; Wen et al., 2014).

EPMA analyses show that Fe concentration of the Geshan dolomite ranges from bdl to 4441.1 ppm (average is 708.4 ppm). The average values are much higher than those for dolomites formed in normal marine environments, which commonly have Fe content between 3 and 50 ppm (Veizer, 1983). The high content of Fe element in dolomite of the Zhouchongcun Formation probably suggests that the dolomites were precipitated from Fe-rich fluids under reducing conditions, or that Fe was preferentially incorporated in the dolomite lattice during burial diagenesis (Kirmaci & Akdag, 2005).

Na contents of dolomites formed in normal marine environment usually range from 110 to 160 ppm (Veizer, 1983; Qing & Mountjoy, 1989). The Na contents of the Geshan dolomite reached 319.03 ppm, and even 712.26 ppm in sample GSN-13 (Fig. 5). Na concentrations can be used as a paleosalinity indicator in ancient carbonates (Veizer et al., 1977). Paleozoic carbonates that formed in hypersaline

environments commonly have higher Na concentrations than their normal marine counterparts (Veizer et al., 1977). The high Na concentration in Geshan dolomite might indicate a high salinity dolomitization fluid. However, the interpretation of Na contents in dolomite is difficult, because high Na content may be due to the occurrence of NaCl liquid or solid inclusions (Qing & Mountjoy, 1989) and to the alteration of Na-bearing clay minerals and tuffites (Kirmaci & Akdag, 2005).

#### 5.4 Interpretation of REE

Seawater REE patterns have hardly changed throughout the Phanerozoic (Shields & Webb, 2004). The signatures of REE+Y patterns and  $\Sigma$ REE+Y barely changed during the dolomitization process (Zhao & Jones, 2013; Wang et al., 2014b). REE patterns of dolomite can serve as a proxy to study the nature of dolomitization fluids and environmental conditions during carbonate precipitation (Zhao & Jones, 2013).

The shale-normalized REE pattern of modern shallow seawater is characterized by obvious negative Ce anomalies, relative enrichment of the heavy REE, positive La anomalies, and high Y/Ho ratios (Fig. 6A) (Shields & Webb, 2004). The shale-normalized REE pattern of Geshan dolomite is characterized by low REE contents and a flat REE pattern (Fig. 6A). No obvious negative Ce anomalies and LREE depletion were observed.

Cerium is redox-sensitive and Ce/Ce\* is a useful proxy to access redox condition under which dolomite precipitated (Zhao & Jones, 2012). The Ce/Ce\* ratios of carbonates from the Zhongchongcun Formation, however, are not compatible with the modern surface seawater (Fig. 6B). Samples show higher Ce/Ce\* ratio and lower Pr/Pr\* ratio than modern shallow seawater. Some other researchers also noticed this phenomenon in study of REE signature of carbonate of Geshan Section and they argued that the obvious positive Ce anomalies in samples than in seawater is due to that Ce prefers to be more enriched in marine carbonate with respect to its REE neighbors La and Pr (Wang et al., 2014b). However, many syn-sedimentary cement and seawater carbonates have negative Ce and positive La anomalies in perfect agreement with modern shallow seawater (Zhao & Jones, 2012; Nothdurft et al., 2004), suggesting there should be other reasons that cause the incompatible Ce anomalies between Geshan carbonates and seawater. In the deep anoxic condition, reduction of Ce<sup>4+</sup> to Ce<sup>3+</sup> would result in an enrichment of dissolved Ce (Mazumdar et al., 1999). The Ce/Ce\* ratios of

carbonates from the Zhongchongcun Formation are higher than surface seawater, indicating a relatively anoxic environment in which these dolomite formed. The Ce/Ce\* ratio of Geshan carbonate increases with burial depth (Fig. 6C), reflecting that the environment becoming more anoxic with the deeper burial depth. The Geshan dolomite does not show obvious LREE depletion, suggesting that the dolomitization fluid were likely rich in LREE relative to seawater. The LREE enrichment may have been caused by continuing degradation of organic matter releasing more LREEs than HREEs into pore water (Haley et al., 2004).

The depth-dependent trend also found in the  $\Sigma\text{REE}+\text{Y}$  content of the carbonate from the Geshan section. The total concentrations of REE+Y in carbonates can be influenced by host rocks, compositions of fluids, and temperatures, etc. (e.g. Qing & Mountjoy, 1994; Kucera et al., 2009). The host limestones were formed from seawater and the REE signature of seawater has not changed throughout the Phanerozoic (Shields & Webb, 2004). Thus, the host rock was not supposed to be a major factor that influenced the  $\Sigma\text{REE}+\text{Y}$  in carbonates of Geshan section. The initial concentrations of REE+Y in fluids are mostly extremely low (from tens of ppm to hundreds of ppb, Douville et al., 1999), which is commonly assumed to be of minor importance for resulting REE+Y patterns of dolomite (Kucera et al., 2009). The temperature of fluid has been documented having a significant influence on the fluid-rock interaction and total REE concentrations (e.g. Qing & Mountjoy, 1994). Dolomites precipitated from fluids with high temperature are mostly REE+Y enriched (Kucera et al., 2009). The depth-dependent trend of  $\Sigma\text{REE}+\text{Y}$  of the carbonate from Zhongchongcun Formation (Fig. 6C) is most likely due to the increasing of temperature as a faction of geothermal gradient.

## 5.5 Interpretation of dolomitization

Considering the petrographic evidence, trace element, REE and isotope data, the dolomite in the Geshan section is best interpreted to have formed in the subsurface during mechanical compaction and early chemical compaction at shallow to intermediated burial. This is indicated by the following evidences: (1) Dolomites commonly contain residual calcites inclusion in their crystals, indicating that these dolomite formed by replacement instead of primary precipitation; (2) Extensive dolomite postdate the stylolitization, indicating that most of the dolomitization occurred at burial depth of more than 500m (Qing & Mountjoy, 1989; Kirmaci & Akdag, 2005); (3) the Geshan dolomite has depleted of  $\delta^{18}\text{O}$  values and low Sr but high Fe, Mn concentration and Ce/Ce\* ratios, suggesting that dolomitization occurred in an anoxic subsurface environment with increasing temperature and burial depth.

### 5.5.1 Sources of magnesium

There are several possible sources of dolomitizing fluids for dolomite formed during shallow to intermediate burial, including: (1) stabilization of high-Mg calcites (e.g. Machel & Anderson, 1989); (2) structural Mg expelled during clay mineral transformation (illitization of smectite) (e.g. Warren, 2000); (3) formation waters (modified seawater, connate seawater preserved in formations) (e.g. Kirmaci & Akdag, 2005).

Stabilization of high Mg-calcite components was probably of no importance in the Zhouchongcun Formation, because most high-Mg calcite had already been transformed to low-Mg calcite before pervasive dolomitization (Machel & Anderson, 1989).

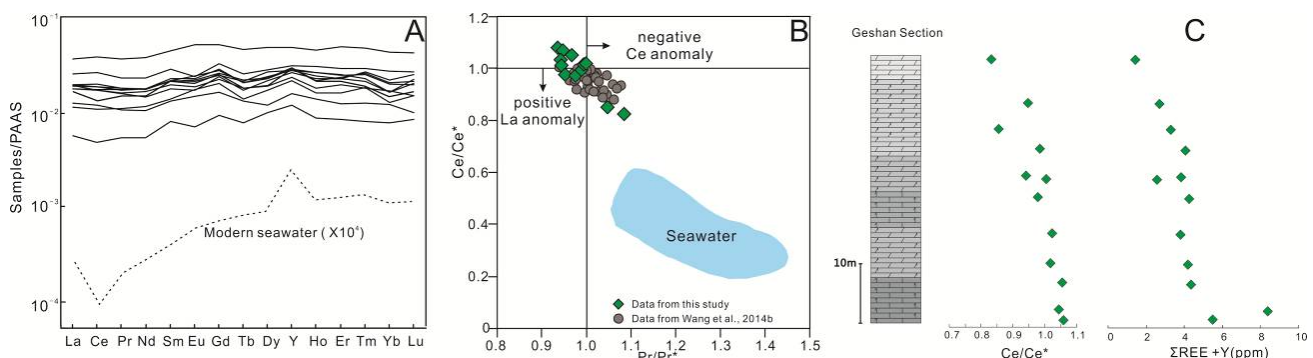


Figure 6. (A) Shale-normalized REE patterns of the Geshan dolomite (solid lines) and modern seawater (dashed line); (B) Cross plot showing relationship between Ce/Ce\* and Pr/Pr\* using the method of Bau et al., 1997. Shaded area shows the range of modern seawater (after Nothdurft et al., 2004); (C) Composite section showing variation in  $\Sigma\text{REE}+\text{Y}$  and Ce/Ce\* of carbonates with depth.

The illitization of smectite could release magnesium into basinal brines and has been considered by many researchers to be a possible source of magnesium to dolomitize adjacent carbonates (Warren, 2000). The Lower and Middle Triassic strata in the study area, however, are mainly composed of carbonate with minor detrital sediments (Wang et al., 2014b) and no clay beds have been observed stratigraphically below or near the Zhouchongcun Formation (Fig. 1B). Since smectites and illite, potential sources of Mg during burial, were very rare, structurally Mg in clay minerals for dolomitization is unlikely in the Zhouchongcun Formation.

Formation waters appear to be the most likely sources of the dolomitizing fluids for the Zhouchongcun Formation. The geochemistry of the dolomite suggests that the water from which the dolomite precipitated were coeval seawater modified by rock-water interaction. These formation waters could have been expelled during mechanical compaction from intermediate to shallow burial depths (Machel & Anderson, 1989; Kirmaci & Akdag, 2005) or migrated laterally from adjacent strata conducted via porous conduits (Qing & Mountjoy, 1989).

### 5.5.2 Timing of dolomitization

As documented earlier, the dolomite of the Zhouchongcun Formation postdates the onset of stylolite development, which commonly begins to occur at the depth of about 500-1000 m.

The dolomite-precipitated temperatures can be estimated if the  $\delta^{18}\text{O}$  value of dolomitizing fluid is known. As the dolomitizing fluids was modified Triassic seawater, we assume that the  $\delta^{18}\text{O}$  value of dolomitizing fluids were similar to the Triassic seawater.  $\delta^{18}\text{O}$  values of marine low-magnesium calcite shells are commonly used to constrain the  $\delta^{18}\text{O}$  of coeval seawater (Land 1983). The low-magnesium shells in Triassic show  $\delta^{18}\text{O}$  values in a range predominantly between -1‰ (V-PDB) and -5‰ (V-PDB) (Veizer et al., 1999).

Assuming that, during the deposition of these marine carbonates in the Lower Yangtze region, the average temperature for the subtropical seawater was 20°C, the calculated  $\delta^{18}\text{O}$  value of the Triassic seawater was approximate between 0.0‰ (SMOW) and -4.1‰ (SMOW), using the Friedman & O'Neil (1977) calcite-water oxygen isotope fractionation equation:

$$1000\ln\alpha_{\text{calcite-water}}=2.78\times 10^6\cdot T^{-2}-2.89.$$

A temperature range between 50°C and 80°C during dolomitization is calculated (Fig. 7), using

the dolomite-water oxygen isotope fraction of Land (1983):  $1000\ln\alpha_{\text{dolomite-water}}=3.2\times 10^6\cdot T^{-2}-3.3$ .

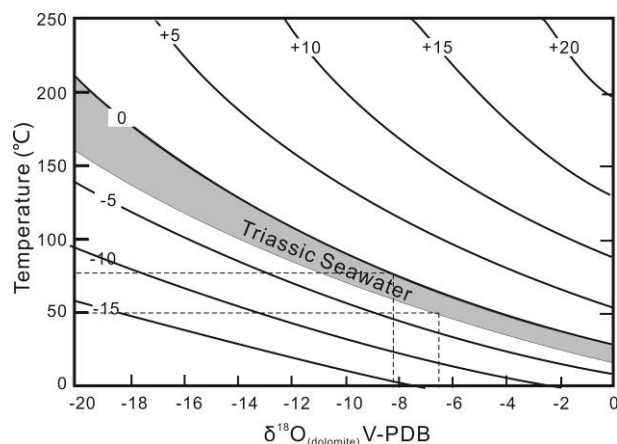


Figure 7. Crossplots of temperature against oxygen isotopic signature for Geshan dolomite in the Zhouchongcun Formation.

Using a surface temperature of 30°C (Qing & Mountjoy, 1989) and geothermal gradient of 3.1°C/100m (Liu, 2004), these temperatures suggest that these dolomites formed at burial depth between 650 and 1600 m. According to the burial history of the Middle Triassic carbonates in the study area, the dolomitization may have taken place during the Late Triassic period (Fig. 8).

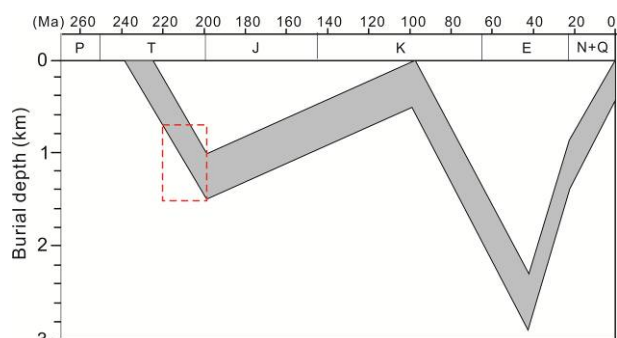


Figure 8. Burial history of Zhouchongcun Formation on the Lower Yangtze region (modified after Li et al., 2013; Liu, 2004), and presumable dolomitization time.

## 6. CONCLUSIONS

Based on petrographic and geochemical investigations of the Geshan dolomites in the Zhouchongcun Formation from the Lower Yangtze region, the following conclusions are drawn:

1) The dolomite commonly displays planar-e texture and locally planar-s texture with crystal sizes less than 80µm. Some dolomites contain residual calcites inclusion in their crystals. Extensive dolomite clearly postdates the onset of stylolite development.

2) Dolomitization occurred in an anoxic subsurface environment with increasing temperature

during mechanical compaction and early chemical compaction at shallow to intermediated burial.

3) The dolomitization mostly occurred during Late Triassic and the main source of dolomitizing fluid was derived from modified seawater of Triassic preserved in formation.

#### Acknowledgements

This study was financially supported by the National Science and Technology Special (Grant No. 2011ZX05009 - 002, No. 2008ZX05005 - 002 - 007HZ).

#### REFERENCES

- Azmy, K., Veizer, J., Misi, A., de Oliveira, T.F., Sanches, A.L., & Dardenne, M.A., 2001. *Dolomitization and isotope stratigraphy of the Vazante Formation, Sao Francisco Basin, Brazil*. Precambrian Research 112, 303-329.
- Barnaby, R.J., & Read, J.F., 1992. *Dolomitization of a carbonate platform during late burial: Lower to Middle Cambrian shady dolomite, Virginia Appalachians*. Journal of Sedimentary Research 62, 1023-1043.
- Bau, M., Moller, P., & Dulski, P., 1997. *Yttrium and lanthanides in eastern Mediterranean sea water and their fractionation during redox-cycling*. Marine Chemistry 56, 123-131.
- Bristow, T.F., Kennedy, M.J., Morrison, K.D., & Mrofka, D.D., 2012. *The influence of authigenic clay formation on the mineralogy and stable isotopic record of lacustrine carbonates*. Geochimica et Cosmochimica Acta 90, 64-82.
- Davies, G.R., & Smith, L.B., 2006. *Structurally controlled hydrothermal dolomite reservoir facies: An overview*. AAPG Bulletin 90, 1641-1690.
- Douville, E., Bienvenu, P., Charlou, J.L., Donval, J.P., Fouquet, Y., Appriou, P., & Gamo, T., 1999. *Yttrium and rare earth elements in fluids from various deep-sea hydrothermal systems*. Geochimica et Cosmochimica Acta 63, 627-643.
- Driese, S.G., & Mora, C.L., 1993. *Physico-chemical environment of pedogenic carbonate formation in Devonian vertic palaeosols, central Appalachians, USA*. Sedimentology 40, 199-216.
- Fookes, E., 1995. *Development and eustatic control of an Upper Jurassic reef complex (Saint Germain-de-Joux, eastern France)*. Facies 33, 129-149.
- Friedman, I. & O'Neil, J.R., 1977. *Compilation of stable isotope fractionation factors of geochemical interest*. In: Fleischer, M. (Eds.), Data of Geochemistry. pp. KK1-KK12, U.S. Geological Survey Professional Paper, 440-KK.
- Haley, B.A., Klinkhammer, G.P., & McManus, J., 2004. *Rare earth elements in pore waters of marine sediments*. Geochimica et Cosmochimica Acta 68, 1265-1279.
- Hu, G.M., Ji, Y.L., Cai, J.G., Lao, Q.Y., & Zhou, Y., 2008. *Tectonic significance of differences anhydrock layers in T1-2 in Lower Yangtze region*. Natural Gas Industry 28, 1-3 (in Chinese).
- Huang, Y., Zhang, Z., Wu, L., Zang, C., & Li, Q., 2012. *Geochemistry and geological significance of the Upper Paleozoic and Mesozoic source rocks in the Lower Yangtze region*. Chinese Journal of Geochemistry 31, 315-322.
- Jimenez-Lopez, C., Romanek, C.S., & Caballero, E., 2006. *Carbon isotope fractionation in synthetic magnesian calcite*. Geochimica et cosmochimica acta, 70, 1163-1171.
- Jones, G.D., & Xiao, Y., 2005. *Dolomitization, anhydrite cementation and porosity evolution in a reflux system: insights from reactive transport models*. AAPG Bulletin 89, 577-601.
- Kirmaci, M.Z., & Akdag, K., 2005. *Origin of dolomite in the Late Cretaceous-Paleocene limestone trubidites, Eastern Pontides, Turkey*. Sedimentary Geology 181, 39-57.
- Korte, C., Kozur, H.W., Bruckschen, P., & Veizer, J., 2003. *Strontium isotope evolution of Late Permian and Triassic seawater*. Geochimica et Cosmochimica Acta 67, 47-62.
- Kucera, J., Cempirek, J., Dolnicek, Z., Muchez, P., & Prochaska, W., 2009. *Rare earth elements and yttrium geochemistry of dolomite from post-Variscan vein-type mineralization of the Nizky Jesenik and Upper Silesian Basins, Czech Republic*. Journal of Geochemical Exploration 103, 69-79.
- Land, L.S., 1983. *The application of stable isotopes to studies of the origin of dolomite and to problems of diagenesis of clastic sediments*. In: Arthur, M.A., Anderson, T.F., Kaplan, I.R., Veizer, J., Land, L.S., (Eds.), Stable Isotopes in Sedimentary Geology. SEPM Short Course Notes 10, 4-1-4-22.
- Land, L.S., 1985. *The origin of massive dolomite*. Journal of Geological Education 33, 112-125.
- Land, L.S., 1991. *Dolomitization of the Hope Gate Formation (north Jamaica) by seawater: reassessment of mixing zone dolomite*. In: Taylor, H.P., O'Neil, J.R., Kaplan, I.R. (Eds.), Stable Isotope Geochemistry: A Tribute to Samuel Epstein. Geochemical Society Special Publication 3, pp. 121-133.
- Li, J., Xia, Z., Shi, H., Hua, C., & Wang, X., 2013. *Characteristics of fluid inclusions and timing of hydrocarbon accumulation in Longtan reservoirs in Huangqiao region, Lower Yangtze Basin*. Petroleum Geology & Experiment 35, 195-198 (in Chinese with English abstract).
- Lind, I.L., 1993. *Stylolites in chalk from Leg, Ontong java Plateau*. In: Berger, W.H., Kroenk, J.W., Mayer, L.A., et al., (Eds.), Proceeding of the Ocean Drilling Program Scientific Results 130, pp. 445-451.
- Liu, D.Y., 2004. *The forming of Mesozoic-Paleozoic marine oil and gas Lower Yangtze river, Jiangsu Province*. Doctoral dissertation, Guangzhou Institute of Geochemistry, Chinese Academy of

- Sciences (In Chinese with English abstract).
- Liu, Z., Tong, J.**, 2001. *The Middle Triassic stratigraphy and sedimentary paleogeography of South China*. *Acta Sedimentologica Sinica* 19, 327-332 (in Chinese with English abstract).
- Ma, Y.S., Guo, T.L., Zao, X.F., & Cai, X.Y.**, 2008. *The formation mechanism of high-quality dolomite reservoir in the deep of Puguang Gas Field*. *Science in China D Earth Sciences* 51, 53-64.
- Machel, H.G., & Anderson, J.H.**, 1989. *Pervasive subsurface dolomitization of the Nisku Formation in central Alberta*. *Journal of Sedimentary Petrology* 59, 891-911.
- Mackenzie, J.**, 1981. *Holocene dolomitization of calcium carbonate sediments from the coastal sabkhas of Abu Dhabi, U.A.E*. *Journal of Geology* 89, 185-198.
- Mazumdar, A., Banerjee, D.M., Schidlowski, M., & Balaram, V.**, 1999. *Rare-earth elements and stable isotope geochemistry of early Cambrian chert-phosphorite assemblages from the Lower Tal Formation of the Krol Belt (Lesser Himalaya, India)*. *Chemical Geology* 156, 275-297.
- Mresah, M.H.**, 1998. *The massive dolomitization of platformal and basinal sequences: proposed models from the Paleocene, northeast Sirte Basin, Libya*. *Sedimentary Geology* 116, 199-226.
- Nothdurft, L.D., Webb, G.E., & Kamber, B.S.**, 2004. *Rare earth element geochemistry of Late Devonian reefal carbonate, Canning Basin, Western Australia: confirmation of seawater REE proxy in ancient limestones*. *Geochimica et Cosmochimica Acta* 68, 263-283.
- Qing, H., & Mountjoy, E.W.**, 1989. *Multistage dolomitization in rainbow buildups, Middle Devonian Keg River Formation, Alberta, Canada*. *Journal of Sedimentary Petrology* 59, 114-126.
- Qing, H., & Mountjoy, E.W.**, 1994. *Rare earth element geochemistry of dolomites in the Middle Devonian Presqu'île barrier, Western Canada Sedimentary Basin: implications for fluid-rock ratios during dolomitization*. *Sedimentology* 41, 787-804.
- Shields, G.A., & Webb, G.E.**, 2004. *Has the REE composition of seawater changed over geological time?* *Chemical Geology* 204, 103-107.
- Smith, L.B.**, 2006. *Origin and reservoir characteristics of Upper Ordovician Trenton-Black River hydrothermal dolomite reservoirs in New York*. *AAPG Bulletin* 90, 1691-1718.
- Sun, S.Q.**, 1995. *Dolomite reservoirs: porosity evolution and reservoir characteristics*. *AAPG Bulletin* 79, 186-204.
- Taylor, S.R., & McLennan, S.M.**, 1985. *The Continental Crust: Its Composition and Evolution*. Blackwell Scientific Publications, Oxford. pp. 312.
- Tritlla, J., Cardellach, E., & Sharp, Z.D.**, 2001. *Origin of vein hydrothermal carbonates in Triassic limestones of the Espadan Ranges (Iberian Chain, E Spain)*. *Chemical Geology* 172, 291-305.
- Veizer, J.**, 1983. *Chemical diagenesis of carbonates: theory and application of trace element technique*. In: Arthur, M.A., Anderson, T.F., Kaplan, I.R., Veizer, J., Land, L.S., (Eds.), *Stable Isotopes in Sedimentary Geology*, SEPM Short Course, vol. 10, pp. 3-1-3-100.
- Veizer, J., Ala, D., Azmy, K., Bruckschen, P., Buhl, D., Bruhn, F., Carden, G., Diener, A., Ebner, S., Goddard, Y., Jasper, T., Korte, C., Pawellek, F., Podlaha, O., & Strauss, H.**, 1999.  *$^{87}\text{Sr}/^{86}\text{Sr}$ ,  $\delta^{18}\text{O}$  and  $\delta^{13}\text{C}$  evolution of Phanerozoic seawater*. *Chemical Geology*, 161, 59-88.
- Veizer, J., Lemieux, J., Jones, B., Gibling, M.R., & Savelle, J.**, 1977. *Sodium: Paleosalinity indicator in ancient carbonate rocks*. *Geology*, 177-179.
- Wang, H.W., & Duan, H.L.**, 2009. *Sedimentary facies of Qinglong Formation in Lower Yangtze region*. *Complex Hydrocarbon Reservoirs* 2, 5-10 (in Chinese with English abstract).
- Wang, L.C., Hu, W.X., & Wang, X.L.**, 2014a. *Dolomitization process and its effect on the behavior of trace elements of carbonate rocks from Triassic Zhouchongcun Formation of Geshan section in Yixing County, Lower Yangtze*. *Geochimica*, in press (in Chinese with English abstract).
- Wang, L.C., Hu, W.X., & Wang, X.L.**, 2014b. *Seawater normalized REE patterns of dolomites in Geshan and Panlongdong sections, China: Implication for tracing dolomitization and diagenetic fluids*. *Marine and Petroleum Geology*, in press.
- Warren, J.**, 2000. *Dolomite: occurrence, evolution and economically important associations*. *Earth Science Reviews* 52, 1-81.
- Wen, H., Wen, L., Chen, H., Zheng, R., Dang, L., & Li, Y.**, 2014. *Geochemical characteristics and diagenetic fluids of dolomite reservoirs in the Huanglong Formation, Eastern Sichuan Basin, China*. *Petroleum Science* 11, 52-66.
- Wierzbicki, R., Dravis, J.J., Al-Aasm, I., & Harland, N.**, 2006. *Burial dolomitization and dissolution of Upper Jurassic Abenaki platform carbonates, Deep Panuke reservoir, Nova Scotia, Canada*. *AAPG Bulletin* 90, 1843-1861.
- You, X.L., Sun, S., Zhu, J.Q., Li, Q., Hu, W.X., Dong, & H.L.**, 2013. *Microbially mediated dolomite in Cambrian stromatolites from the Tarim Basin, north-west China: implication for the role of organic substrate on dolomite precipitation*. *Terra Nova* 25, 387-395.
- Zhao, H., & Jones, B.**, 2012. *Origin of "island dolostones": A case study from the Caman Formation (Miocene), Cayman Brac, British West Indies*. *Sedimentary Geology* 243, 191-206.
- Zhao, H., & Jones, B.**, 2013. *Distribution and interpretation of rare earth elements and yttrium in Cenozoic dolomites and limestones on Cayman Brac, British West Indies*. *Sedimentary Geology* 284, 26-38.

Received at: 30. 07. 2014  
Revised at: 25. 11. 2014  
Accepted for publication at: 05. 12. 2014  
Published online at: 10. 12. 2014